Phytochemistry Letters 14 (2015) 215–220

Contents lists available at ScienceDirect

Phytochemistry Letters

journal homepage: www.elsevier.com/locate/phytol

Two new phenolic compounds from the white flower of *Impatiens balsamina*

Chung Sub Kim[a], Lalita Subedi[b,c], Sun Yeou Kim[b,c], Sang Un Choi[d], Sang Zin Choi[e], Mi Won Son[e], Ki Hyun Kim[a], Kang Ro Lee[a,*]

[a] Natural Products Laboratory, School of Pharmacy, Sungkyunkwan University, Suwon 16419, Republic of Korea
[b] Gachon Institute of Pharmaceutical Science, Gachon University, Incheon 21936, Republic of Korea
[c] College of Pharmacy, Gachon University, Incheon 21936, Republic of Korea
[d] Korea Research Institute of Chemical Technology, Daejeon 34114, Republic of Korea
[e] Dong-A ST Research Institute, Kiheung, Yongin 17073, Republic of Korea

ARTICLE INFO

Article history:
Received 28 August 2015
Received in revised form 1 October 2015
Accepted 19 October 2015
Available online xxx

Keywords:
Impatiens balsamina
Balsamineaceae
Phenolic compounds
Cytotoxicity
Neuroprotection
Anti-neuroinflammation

ABSTRACT

During the course of our continuing search for biologically active compounds from Korean medicinal sources, we investigated the white flower of *Impatiens balsamina*. From the MeOH extract, two new phenolic compounds (**1**–**2**) containing a nitrile group and eleven known phenolic compounds (**3**–**13**) were isolated. The chemical structures of new compounds (**1**–**2**) were determined through NMR, HRMS, and CD data. We tested the isolated compounds (**1**–**13**) for their cytotoxic activities by determining their inhibitory effects on human tumor cell lines (A549, SK-OV-3, SK-MEL-2, and HCT15) *in vitro* using the sulforhodamine B (SRB) assay. We also investigated their neuroprotective activity by determining their effects on nerve growth factor (NGF) secretion in C6 cells, and anti-neuroinflammatory activity by measuring nitric oxide (NO) production in lipopolysaccharide (LPS)-stimulated BV-2 cells.

1. Introduction

Impatiens balsamina L., also known as Garden balsam or Rose balsam, is an annual herbaceous plant of the Balsamineaceae family grown as an ornamental garden plant. *I. balsamina*has been used in traditional Chinese medicine, and in some areas of China is used as a vegetable or anticancer herb (Su et al., 2012). The aerial parts of *I. balsamina*have been used for the treatment of articular rheumatism, bruises, and beriberi (Imam et al., 2012), whereas the seeds have been used to treat lumps, puerperal pain, and cancer (Lei et al., 2010). The flower of this plant also has been used to treat dermititis, lumbago, neuralgia, burns, and scalds (Imam et al., 2012). Previous studies have suggested that flavonoids and naphthoquinones from the flower of *I. balsamina*are associated with antipruritic, antianaphylactic, and anti-inflammatory properties (Fukumoto et al., 1996; Ishiguro and Oku, 1997; Oku and Ishiguro, 2002). As part of the searching for bioactive constituents of Korean medicinal plant sources, we investigated the active constituents of *I. balsamina*. In the present study, we report the isolation and structural elucidation of two new phenolic compounds (**1** and **2**) and eleven known compounds (**3**–**13**) (Fig. 1), from the white flower of*I. balsamina*. We also determined their anticancer effects on human tumor cell lines (A549, SK-OV-3, SK-MEL-2, and HCT15) *in vitro* using the sulforhodamine B (SRB) assay, their neuroprotective activity by determining their effects on nerve growth factor (NGF) secretion in C6 cells, and their anti-neuroinflammatory activity by measuring nitric oxide (NO) production in lipopolysaccharide (LPS)-stimulated BV-2 cells.

2. Results and discussion

Compound **1** was isolated as a colorless gum. The molecular formula was determined as $C_{10}H_7NO_3$ from the pseudomolecular ion peak $[M+H]^+$ at *m/z*190.0557 (calcd for $C_{10}H_8NO_3$, 190.0504) in the HRESIMS. The IR spectrum of **1** displayed absorption bands at 3433 (hydroxyl) and 2243 (nitrile) cm^{-1}. The ^1H NMR spectrum of **1** exhibited the presence of a 1,2-disubstituted aromatic ring [δ_H 7.57 (1H, d, *J* = 7.5 Hz), 7.35 (1H, t, *J* = 7.5 Hz), 7.13 (1H, t, *J* = 7.5 Hz), and 6.96 (1H, d, *J* = 7.5 Hz)] and a methylene group [δ_H 3.10 (1H, d, *J* = 16.6 Hz) and 2.90 (1H, d, *J* = 16.6 Hz)]. The ^{13}C NMR spectrum of **1** showed 10 carbon signals including a carbonyl carbon (δ_C 179.4), six

* Corresponding author at: Natural Products Laboratory, School of Pharmacy, Sungkyunkwan University, 2066 Seobu-ro, Jangan-ku, Suwon 16419, Republic of Korea. Fax: +82 31 290 7730.
E-mail address: krlee@skku.edu (K.R. Lee).

http://dx.doi.org/10.1016/j.phytol.2015.10.014
1874-3900/

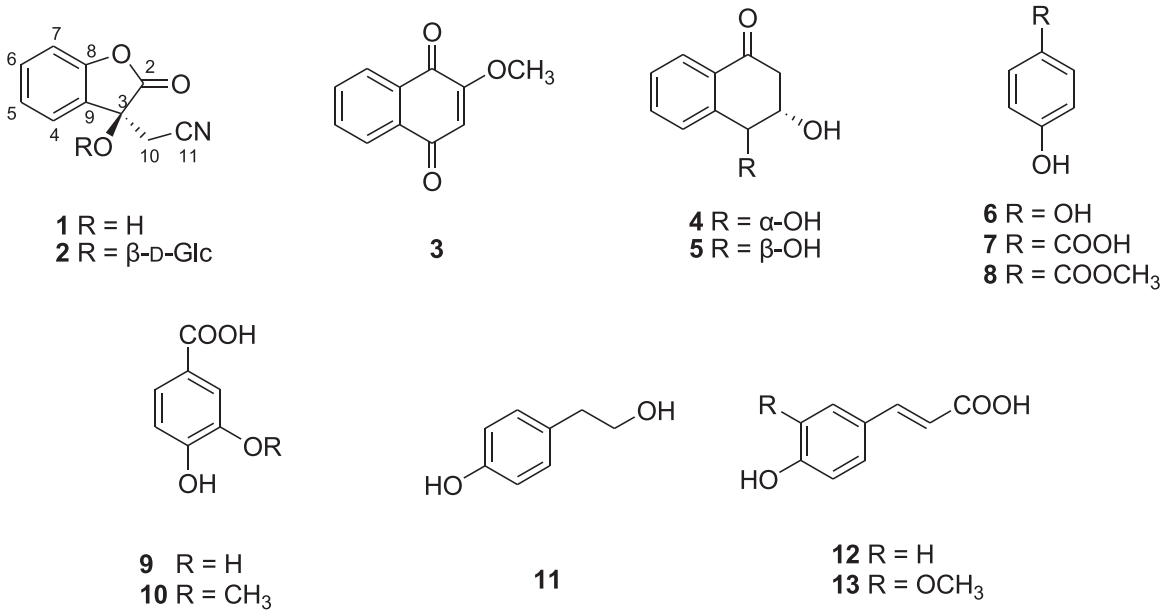

Fig. 1. Chemical structures of compounds **1**–**13**.

aromatic carbons [δ_C 142.9, 131.7 (×2), 125.5, 124.1, and 111.7], a nitril carbon (δ_C 117.4), an oxygenated carbon (δ_C 74.1), and an alkane carbon (δ_C 27.4). These NMR data of **1** (Table 1) were very similar to those of (−)-(*S*)-2-(4-hydroxy-2-oxo-2,3-dihydrobenzofuran-3-yl) acetonitrile (Zhang et al., 2014), except for the presence of four aromatic proton signals and an oxygenated carbon signal in **1** instead of three aromatic proton signals [δ_H 7.09 (1H, dd, *J* = 8.4, 7.8 Hz), 6.50 (1H, d, *J* = 8.4 Hz), and 6.44 (1H, d, *J* = 7.8 Hz)] and a methine carbon (δ_C 42.3) signal in (−)-(*S*)-2-(4-hydroxy-2-oxo-2,3-dihydrobenzofuran-3-yl) acetonitrile. The ^{1}H–^{1}H COSY correlations from H-4 to H-7 and the HMBC cross-peaks of H-5/C-9, H-6/C-8, and H-7/C-9 confirmed the substructure of unit A (Fig. 2). The HMBC cross-peaks of H-10/C-2, C-3, and C-11 suggested two possible substructures, unit B1 and B2 (Fig. 2). However, in the case of unit B2, the chemical shift of C-10 was expected to be at δ_C 40 from the inspection of related compounds (Xie and Stahl, 2015; Yuan et al., 2009), which was quite different from that of the experimental value (δ_C 27.4). Therefore, the only possible substructure was unit B1. Direct linkage between C-3 and C-9 was confirmed through the HMBC correlations of H-4/C-3 and H-10/C-9, and the relatively downfield shifted chemical shift of C-8 (δ_C 142.9) corroborated that C-8 was connected to the oxygen atom adjacent to C-2. The absolute configuration at C-3 was determined through the CD spectrum of **1** (Fig. 3). The strong negative Cotton effect at 236 nm in **1** was opposite to that of (−)-(*S*)-2-(4-hydroxy-2-oxo-2,3-dihydrobenzofuran-3-yl) acetonitrile (Zhang et al., 2014), which confirmed the absolute configuration at C-3 in **1** to be the *S*form. Therefore, the structure of **1** was established as (*S*)-2-(3-hydroxy-2-oxo-2,3-dihydrobenzofuran-3-yl) acetonitrile, named balsamitril.

Table 1
1H (700 MHz) and ^{13}C (175 MHz) NMR data of compounds **1** and **2** in CD_3OD (δin ppm, *J*values in parentheses).

Pos.	**1**		**2**	
	δ_H	δ_C	δ_H	δ_C
2		179.4		176.5
3		74.1		79.8
4	7.57, d (7.5)	125.5	7.72, d (7.5)	127.9
5	7.13, t (7.5)	124.1	7.12, t (7.5)	124.0
6	7.35, t (7.5)	131.7	7.37, t (7.5)	132.5
7	6.96, d (7.5)	111.7	6.96, d (7.5)	112.0
8		142.9		143.8
9		131.7		126.4
10a	3.10, d (16.6)	27.4	3.33, d (16.6)	27.0
10b	2.90, d (16.6)		3.14, d (16.6)	
11		117.4		117.0
1′			4.24, d (7.5)	101.3
2′			3.24, overlap	74.9
3′			3.21, overlap	78.0
4′			3.26, overalp	71.4
5′			2.97, ddd (9.5, 5.7, 2.5)	78.1
6′a			3.71, dd (11.9, 2.5)	62.7
6′b			3.57, dd (11.9, 5.7)	

Compound **2** was obtained as a colorless gum. The HRESIMS data (*m*/*z*352.1049 [M + H]$^+$, calcd for $C_{16}H_{18}NO_8$, 352.1032) of **2** indicated that this molecule possessed the molecular formula $C_{16}H_{17}NO_8$. The ^{1}H and ^{13}C NMR spectra of **2** were very similar to those of **1**, except for the presence of a D-glucosyl unit [δ_H 4.24 (1H, d, *J* = 7.5 Hz), 3.71 (1H, dd, *J* = 11.9, 2.5 Hz), 3.57 (1H, dd, *J* = 11.9, 5.7 Hz), 3.26 (1H, overlap), 3.24 (1H, overlap), 3.21 (1H, overlap), and 2.97 (1H, ddd, *J* = 9.5, 5.7, 2.5 Hz); δ_C 101.3, 78.1, 78.0, 74.9, 71.4, and 62.7]. The location of the glucosyl unit was confirmed at C-3 through the HMBC cross-peak of H-1′/C-3 (Fig. 2). Enzymatic hydrolysis of **2** yielded the aglycone **2a**, which was identified as **1** by comparing the ^{1}H NMR and ESIMS data with those of **1**. Identification of D-glucose was performed through the acid hydrolysis of **2**, followed by co-TLC confirmation with authentic sample, specific optical rotation {([α]^{25}D + 59.8) (*c*0.05, H_2O)}, and GC/MS analysis. The absolute configuration at C-3 in **2** was determined to be *S*by the same method as **1** (see Supplementary data). Thus, the structure of **2** was elucidated as (*S*)-2-(3-hydroxy-2-oxo-2,3-dihydrobenzofuran-3-yl) acetonitrile-3-*O*-β-D-glucoside, named balsamitril -3-*O*-β-D-glucoside.

The known compounds were identified as 2-methoxy-1,4-naphthoquinone (**3**) (Ding et al., 2008), (3*S*,4*R*)-3,4-dihydroxy-3,4-dihydronaphthalen-1(2*H*)-one (**4**) (Husain et al., 2012), *trans*-(3*S*,4*S*)-3,4-dihydroxy-1-tetralone (**5**) (Husain et al., 2014), hydroquinone (**6**) (Bernini et al., 2005), *p*-hydroxybenzoic acid (**7**) (O'Connor et al., 1987), *p*-hydroxybenzoic acid methyl ester (**8**) (Kwak et al., 2009), protocatechuic acid (**9**) (Kwak et al., 2009), vanilic acid (**10**) (Prachayasittikul et al., 2009), tyrosol (**11**) (Takaya et al., 2007), *trans*-*p*-coumaric acid (**12**) (Salum et al., 2010), and *trans*-ferulic acid (**13**) (Prachayasittikul et al., 2009) by comparison with NMR and MS data in the literature.

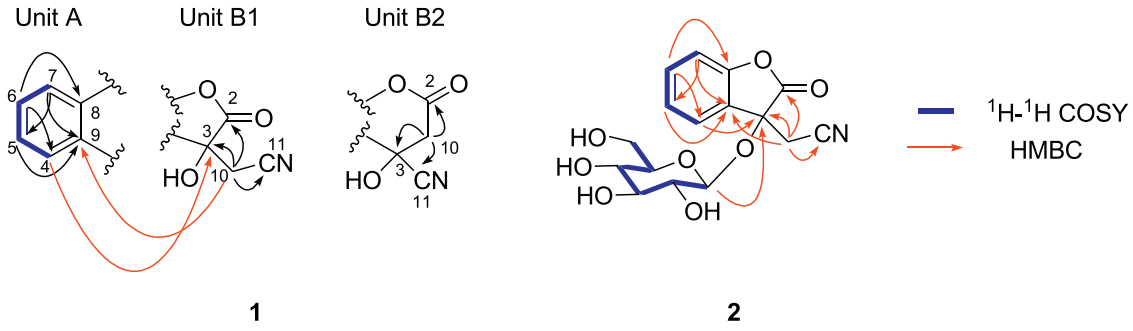

Fig. 2. ^{1}H–^{1}H COSY (bold) and HMBC (arrows) correlations of **1** and **2**.

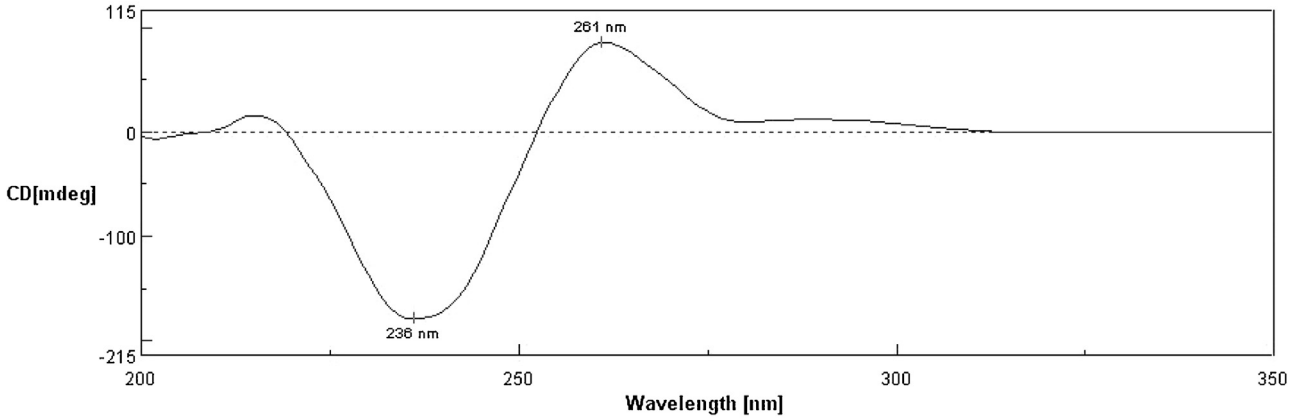

Fig. 3. CD spectrum of compound **1**.

The SRB assay was used to evaluate the antiproliferative activities of the isolated compounds **1**–**13** (Skehan et al., 1990), which were tested against the four human tumor cell lines, A549 (non-small cell lung carcinoma), SKOV-3 (ovarian malignant ascites), SK-MEL-2 (skin melanoma), and HCT15 (colon adenocarcinoma). As shown in Table 2, compounds **3**,**4**, **5**, **6** and **11** showed cytotoxic activities against the SK-MEL-2 cell line with IC_{50} values ranging from 1.03 to 28.71 μM, however the remaining compounds were inactive (IC_{50} > 30.0 μM). Among the active compounds, compound **3** showed the most potent cytotoxic activity against the SK-MEL-2 cell line (IC_{50} 1.03 μM), even better than etoposide, the positive control (IC_{50} 1.33 μM) (Table 2). In addition, compound **3** displayed weak activity against A549 cells with an IC_{50} value of 25.52 μM.

Microglial cells, the immune resident cells of the brain, are principally responsible for immune defense in the central nervous system. However, under pathological conditions, microglia cells are over-activated and then produce a variety of proinflammatory mediators including NO (Chao et al., 1992; McGeer et al., 1993). Compounds with high efficacy in inhibition of NO production might possess potent antineuroinflammatory efficacy. In the present study, we evaluated the effects of the isolated compounds (**1**–**13**) on NO inhibition in lipopolysaccharide (LPS)-stimulated murine microglia BV2 cells (Table 3). Compounds **3**, **6**, and **10** exhibited inhibitory effects on NO production with IC_{50} values of 27.40, 20.73, and 33.70 μM, respectively, without significant cell toxicity at 20 μM. Among those, compound **6** showed the most potent activity (IC_{50} 20.73 μM), which was comparable to that of the positive control, L-NMMA (IC_{50} 20.53 μM).

In neuronal environment, neuroprotection was possible via increased production of neurotrophins like NGF. Compounds that can induce the production on NGF can be the effective neuroprotective agents against LPS induced neuronal death (Tabakman et al., 2005). We tested compounds **1**–**13** for their neuroprotective effects using an enzyme-linked immunosorbent assay (ELISA) development kit to measure NGF release from C6 glioma cells into the medium. Cell viability was assessed using the 3-[4,5-dimethylthiazol-2-yl]-2,5-diphenyl-tetrazolium bromide (MTT) assay. Compounds **1**, **3**, **6**, **8**, **9**, and **12** exhibited a strong induction of NGF secretion by 151.47 ± 4.74%–160.46 ± 5.63%, which was comparable to that of the positive control, 6-shogaol (158.18 ± 6.56%) (Table 4). Compounds **2**, **5**, **7**, **10**, and **13** also increased NGF secretion to 131.30 ± 4.65%–145.67 ± 1.13%, and none of the compounds showed any significant cellular toxicity at 20 μM. Interestingly, compound **1** was more active than its glycoside form, compound **2** (**1**, 155.59 ± 13.21%; **2**, 136.70 ± 6.68%). Moreover, compound **8**, a methyl ester form of compound **7**, induced more NGF secretion than compound **7** (**7**, 131.30 ± 4.65%; **8**, 125.06 ± 4.77%). Although the only structural difference between compound **9** and **10** was the presence of a hydroxyl and methoxyl group at C-3, respectively, compound **9** showed a

Table 2
Cytotoxicity of compounds **3**–**6** and **11** against four cultured human cancer cell lines in the SRB bioassay.

Comp.	IC_{50} (μM)[a]			
	A549	SK-OV-3	SK-MEL-2	HCT15
3	25.51	>30.0	1.03	>30.0
4	>30.0	>30.0	14.83	>30.0
5	>30.0	>30.0	28.71	>30.0
6	>30.0	>30.0	11.78	>30.0
11	>30.0	>30.0	14.38	>30.0
Etoposide[b]	1.74	1.96	1.33	2.95

[a] 50% inhibitory concentration; the concentration of compound that caused a 50% inhibition in cell growth.
[b] Etoposide was used as a positive control.

Table 3
Inhibitory effect of compounds **1**–**13** on NO production in LPS-activated BV-2 cells.

Comp.	IC_{50} (μM)[a]	Cell viability (%)[b]	Comp.	IC_{50} (μM)[a]	Cell viability (%)[b]
1	64.08	97.95 ± 12.23	**8**	79.64	82.43 ± 5.84
2	93.36	90.83 ± 5.77	**9**	81.11	77.10 ± 4.49
3	27.40	151.59 ± 10.71	**10**	33.70	143.36 ± 6.90
4	58.17	142.39 ± 4.08	**11**	240.67	104.89 ± 16.49
5	101.40	98.48 ± 6.60	**12**	74.80	111.07 ± 12.14
6	20.73	107.76 ± 5.14	**13**	155.77	112.11 ± 8.43
7	107.72	88.14 ± 9.74	**L-NMMA**[c]	20.53	100.42 ± 5.16

[a] IC_{50} value of each compound was defined as the concentration (μM) that caused 50% inhibition of NO production in LPS-activated BV-2 cells.
[b] Cell viability following treatment with 20 μM each compound was determined by the MTT assay and is expressed as a percentage (%). Data are expressed as the mean ± SD of three independent experiments.
[c] L-NMMA was used as a positive control.

Table 4
Effects of compounds **1**–**13** on NGF secretion in C6 cells.

Comp.	NGF secretion (%)[a]	Cell viability (%)[b]	Comp.	NGF secretion (%)[a]	Cell viability (%)[b]
1	155.59 ± 13.21	118.35 ± 6.64	**8**	152.06 ± 4.77	108.08 ± 4.70
2	136.70 ± 6.68	112.76 ± 4.66	**9**	160.46 ± 5.63	113.79 ± 3.67
3	151.47 ± 4.74	115.43 ± 2.00	**10**	135.23 ± 10.12	125.90 ± 0.13
4	102.81 ± 3.05	118.26 ± 1.65	**11**	109.47 ± 6.14	116.81 ± 1.49
5	137.38 ± 4.81	124.26 ± 0.45	**12**	154.49 ± 2.89	113.78 ± 0.16
6	157.19 ± 1.49	108.73 ± 5.49	**13**	145.67 ± 1.13	119.44 ± 2.36
7	131.30 ± 4.65	105.21 ± 3.83	**6-Shogaol** [c]	158.18 ± 6.56	109.83 ± 4.64

[a] C6 cells were treated with 20 μM compounds. After 24 h, the amount of NGF secreted in C6-conditioned media was measured by ELISA. The level of secreted NGF is expressed as a percentage of the untreated control (set as 100%). Data are the mean ± SD of three independent experiments performed in triplicate.
[b] Cell viability following treatment with 20 μM each compound was determined by the MTT assay and is expressed as a percentage (%). Data are expressed as the mean ± SD of three independent experiments.
[c] 6- Shogaol was used as a positive control.

higher inductive activity in NGF secretion than compound **10** (**9**, 160.46 ± 5.63%; **10**, 135.23 ± 10.12%).

3. Experimental

3.1. General experimental procedures

Optical rotation was measured on a Jasco P-1020 polarimeter (Jasco, Easton, MD, USA). Infrared (IR) spectra were recorded on a Bruker IFS-66/S Fourier-transform IR spectrometer (Bruker, Karlsruhe, Germany). Ultraviolet (UV) spectra were recorded with a Shimadzu UV-1601 UV–visible spectrophotometer (Shimadzu, Tokyo, Japan). CD spectra were recorded with a JASCO J-810 spectropolarimeter (Jasco, Tokyo, Japan). HRESIMS was conducted on a Waters SYNAPT G2 (UK). NMR spectra were recorded on a Bruker AVANCE III 700 NMR spectrometer at 700 MHz (^{1}H) and 175 MHz (^{13}C). The preparative high performance liquid chromatography (HPLC) system had a Gilson 306 pump (Middleton, WI, USA) with a Shodex refractive index detector (New York, NY, USA). Column chromatography was performed with silica gel 60 (70–230 and 230–400 mesh; Merck, Darmstadt, Germany) and RP-C_{18} silica gel (Merck, 230–400 mesh). LPLC was performed over a LiChroprep Lobar-A Si 60 column (Merck, 240 mm × 10 mm i.d.) equipped with an FMI QSY-0 pump. Sephadex LH-20 (Pharmacia Co. Ltd.) was used as a packing material for molecular sieve column chromatography. Merck precoated silica gel F_{254} plates and reversed-phase (RP)-18 F_{254s} plates (Merck) were used for thin-layer chromatography (TLC). Spots were detected on TLC under UV light or by heating after spraying the samples with anisaldehyde-sulfuric acid.

3.2. Plant material

The white flower of *I. balsamina*were collected in Asan, Korea, in August 2014, and the plant was identified by one of the authors (K.R.L.). A voucher specimen (SKKU-NPL 1406) was deposited in the herbarium of the School of Pharmacy, Sungkyunkwan University, Suwon, Korea.

3.3. Extraction and isolation

The white flower of *I. balsamina*(3.0 kg) were extracted with 80% aqueous MeOH at room temperature and filtered. The filtrate was evaporated under reduced pressure to obtain the MeOH extract (730 g), which was suspended in distilled H_2O and successively partitioned with *n*-hexane, $CHCl_3$, EtOAc, and *n*-butanol, yielding 62, 55, 50, and 86 g residues, respectively. The EtOAc-soluble fraction (20 g) was separated over a silica gel column ($CHCl_3$–MeOH–H_2O, 4:1:0.1) to yield eight fractions (A–H). Fraction B (3.7 g) was chromatographed on a Sephadex LH-20 column (100% MeOH) to give eight subfractions (B1–B8). Fraction B2 (250 mg) was subjected to a RP-C_{18} silica gel column with 50% aqueous MeOH, and further purified by semi-preparative HPLC (2 mL/min, 40% aqueous MeOH) to yield compounds **1** (5 mg), **4** (4 mg), **5** (8 mg), **7** (15 mg), and **11** (4 mg). Fraction B3 (300 mg) was separated over a RP-C_{18} silica gel column with 50% aqueous MeOH and further purified by semi-preparative HPLC (2 mL/min, 30–40% aqueous MeOH) to yield compounds **6** (6 mg), **10** (4 mg), **12** (10 mg), and **13** (8 mg). Fraction D (3.4 g) was chromatographed on a RP-C_{18} silica gel column (60% aqueous MeOH) to yield six subfractions (D1–D6). Fraction D1 (170 mg) was subjected to a Lobar-A RP-C_{18} column with 25% aqueous MeOH, and further purified by semi-preparative HPLC (2 mL/min, 17% aqueous MeOH) to yield compounds **2** (4 mg) and **9** (3 mg). Fraction D3 was separated on a Lobar-A RP-C_{18} column with 50% aqueous MeOH, and further purified by semi-preparative HPLC (2 mL/min, 64% aqueous MeOH) to yield compound **3** (3 mg). Fraction E (1.5 g) was chromatographed on an RP-C_{18} silica gel column (55% aqueous MeOH) to yield nine subfractions (E1–E9).

Compound **8** (2 mg) was obtained from fraction E1 (90 mg) by semi-preparative HPLC (25% aqueous MeOH).

*3.3.1. Balsamitril (**1**)*

Colorless gum; $[\alpha]^{25}_{D}$ − 30.0 (*c*0.06, MeOH); IR (KBr) ν_{max} cm^{-1}: 3433, 2243, 1699, 1620, 1457, 1290; UV (MeOH) λ_{max} (log ε) 290 (3.56), 249 (3.88), 220 (4.14) nm; CD (MeOH) λ_{max} ($\Delta\varepsilon$) 261 (+8.87), 236 (−17.12) nm; ^{1}H and ^{13}C NMR data, see Table 1; HRESIMS (positive-ion mode) *m*/*z* 190.0557 $[M+H]^+$ (calcd. for $C_{10}H_8NO_3$, 190.0504).

*3.3.2. Balsamitril-3-O-β-D-glucoside (**2**)*

Colorless gum; $[\alpha]^{25}_{D}$ − 9.7 (*c* 0.02, MeOH); IR (KBr) ν_{max} cm^{-1}: 3434, 2242, 1700, 1625, 1451, 1289; CD (MeOH) λ_{max} ($\Delta\varepsilon$) 260 (+8.11), 235 (−16.98) nm; ^{1}H and ^{13}C NMR data, see Table 1; HRESIMS (positive-ion mode) *m*/*z*352.1049 $[M+H]^+$ (calcd. for $C_{16}H_{18}NO_8$, 352.1032).

*3.4. Enzymatic hydrolysis of **2***

A solution of compound **2** (1.0 mg) in H_2O (2 mL) was hydrolyzed with β-glucosidase (almonds, Sigma) at 37 °C for 24 h. The reaction mixture was extracted with $CHCl_3$ three times to yield 0.5 mg aglycone **2a**, which was identified as **1** by comparing the ^{1}H NMR and ESIMS data with those of **1**.

*3.5. Acid hydrolysis of **2** and sugar analysis*

Compound **2** (1.5 mg) was refluxed with 1 mL of 1 N HCl for 1 h at 90 °C and the hydrolysate was extracted with $CHCl_3$. The aquatic layer was neutralized through an Amberlite IRA-67 column to give the sugar. The sugar obtained from the hydrolysis was dissolved in anhydrous pyridine (0.5 mL) followed by the addition of L-cysteine methyl ester hydrochloride (2 mg) (Sigma). The mixture was stirred at 60 °C for 1.5 h and trimethylsilylated with 1-trimethylsilylimidazole (0.1 mL) (Sigma) for 2 h. The mixture was partitioned between *n*-hexane and H_2O (1 mL each), and the organic layer (1 μL) was analyzed by GC/MS. D-glucose {($[\alpha]^{25}_{D}$ + 59.8) (*c*0.05, H_2O)} was detected by co-injection of the hydrolysate with standard silylated samples, giving a single peak at 9.712 min. Authentic samples (Sigma) treated in the same way showed a single peak at 9.730 min. GC-MS conditions: capillary column, HP-5MS UI (30 m × 0.25 mm × 0.25 μm, Agilent), column temperature, 230 °C; injection temperature, 250 °C; carrier gas, N_2.

3.6. Cytotoxicity assessment

The cytotoxicity of the compounds against cultured human tumor cell lines was evaluated by the SRB method. The assays were performed at the Korea Research Institute of Chemical Technology. Each tumor cell line was inoculated over standard 96-well flat-bottomed microplates, and incubated for 24 h at 37 °C in a humidified atmosphere of 5% CO_2. The attached cells were incubated with serially diluted samples. After 48 h of continuous exposure to the compounds, the culture medium was removed, and the cells were fixed with 10% cold trichloroacetic acid at 4 °C for 1 h. After washing with tap water, the cells were stained with 0.4% SRB dye and incubated for 30 min at room temperature. The cells were washed again and then solubilized with 10 mM unbuffered Tris base solution (pH 10.5). Absorbance was measured spectrophotometrically at 520 nm with a microtiter plate reader. Etoposide (≥98%; Sigma Chemical Co., St. Louis, MO, USA) was used as the positive control. Etoposide had IC_{50} values against A549 (non-small cell lung adenocarcinoma), SK-OV-3 (ovarian malignant ascites), SK-MEL-2 (skin melanoma), and HCT15 (colon adenocarcinoma) of 1.74, 1.96, 1.33, and 2.95 μM, respectively.

3.7. Measurement of NO production and cell viability in LPS-activated BV-2 cells

BV-2 microglia cells were stimulated with 100 ng/mL LPS in the presence or absence of samples for 24 h. Nitrite in the culture media, a soluble oxidation product of NO, was measured by the Griess reaction. Supernatant (50 μL) was harvested and mixed with an equal volume of Griess reagent (1% sulfanilamide, 0.1% *N*-1-napthylethylenediamine dihydrochloride in 5% phosphoric acid). Absorbance at 540 nm was measured after 10 min using a microplate reader (Emax, Molecular Device, Sunnyvale, CA, USA). Graded sodium nitrite solutions were used as standards to calculate the nitrite concentrations in the media. Cell viability was measured using an MTT colorimetric assay. The NO synthase inhibitorN^G-monomethyl-L-arginine (Sigma) was used as a positive control.

3.8. NGF and cell viability assays

C6 glioma cells were used to measure NGF release. C6 cells were purchased from the Korean Cell Line Bank, and maintained in DMEM supplemented with 10% fetal bovine serum (FBS) and 1% penicillin–streptomycin in a humidified incubator with 5% CO_2. C6 cells were seeded into 24-well plates (1×10^5 cells/well) to measure the NGF content in the medium and to assess cell viability. After 24 h, cells were treated with DMEM containing 2% FBS and 1% penicillin–streptomycin with 20 μM each sample for 1 day. The media was used for the NGF ELISA (R&D Systems, Minneapolis, MN, USA). Cell viability was assessed with the MTT assay.

Acknowledgements

This study was supported by a research fund from the Dong-A ST Research Center, 2015. We thank the Korea Basic Science Institute (KBSI) for the MS spectra measurements.

Appendix A. Supplementary data

Supplementary data associated with this article can be found, in the online version, at http://dx.doi.org/10.1016/j.phytol.2015.10.014.

References

Bernini, R., Coratti, A., Provenzano, G., Fabrizi, G., Tofani, D., 2005. Oxidation of aromatic aldehydes and ketones by H_2O_2/CH_3ReO_3 in ionic liquids: a catalytic efficient reaction to achieve dihydric phenols. Tetrahedron 61, 1821–1825.

Chao, C.C., Hu, S., Molitor, T.W., Shaskan, E.G., Peterson, P.K., 1992. Activated microglia mediate neuronal cell injury via a nitric oxide mechanism. J. Immunol. 149, 2736–2741.

Ding, Z.-S., Jiang, F.-S., Chen, N.-P., Lv, G.-Y., Zhu, C.-G., 2008. Isolation and identification of an anti-tumor component from leaves of *Impatiens balsamina*. Molecules 13, 220–229.

Fukumoto, H., Yamaki, M., Isoi, K., Ishiguro, K., 1996. Antianaphylactic effects of the principal compounds from the white petals of *Impatiens balsamina*L. Phytother. Res. 10, 202–206.

Husain, S.M., Schaetzle, M.A., Roehr, C., Luedeke, S., Mueller, M., 2012. Biomimetic asymmetric synthesis of (*R*)-GTRI-02 and (3*S*,4*R*)-3,4-dihydroxy-3,4-dihydronaphthalen-1(2*H*)-ones. Org. Lett. 14, 3600–3603.

Husain, S.M., Schaetzle, M.A., Roehr, C., Luedeke, S., Mueller, M., 2014. Unprecedented role of hydronaphthoquinone tautomers in biosynthesis. Angew. Chem. Int. Ed. 53, 9806–9811.

Imam, M.Z., Nahar, N., Akter, S., Rana, M.S., 2012. Antinociceptive activity of methanol extract of flowers of *Impatiens balsamina*. J. Ethnopharmacol. 142, 804–810.

Ishiguro, K., Oku, H., 1997. Antipruritic effect of flavonol and 1,4-naphthoquinone derivatives from *Impatiens balsamina* L. Phytother. Res. 11, 343–347.

Kwak, J.H., Kim, H.J., Lee, K.H., Kang, S.C., Zee, O.P., 2009. Antioxidative iridoid glycosides and phenolic compounds from *Veronica peregrina*. Arch. Pharm. Res. 32, 207–213.

Lei, J., Qian, S.-H., Jiang, J.-Q., 2010. Two new flavone glycosides from the seeds of *Impatiens balsamina* L. J. Asian Nat. Prod. Res. 12, 1033–1037.

McGeer, P.L., Kawamata, T., Walker, D.G., Akiyama, H., Tooyama, I., McGeer, E.G., 1993. Microglia in degenerative neurological disease. Glia 7, 84–92.
O'Connor, C.J., McLennan, D.J., Calvert, D.J., Mitha, A.S.H., 1987. Substituent effects on the NMR spectra of carboxylic acid derivatives. IV. Carbon-13 NMR spectra of para-substituted phenols, phenylureas and phenyl propionates. Aust. J. Chem. 40, 677–686.
Oku, H., Ishiguro, K., 2002. Cyclooxygenase-2 inhibitory 1,4-naphthoquinones from *Impatiens balsamina*L. Biol. Pharm. Bull. 25, 658–660.
Prachayasittikul, S., Suphapong, S., Worachartcheewan, A., Lawung, R., Ruchirawat, S., Prachayasittikul, V., 2009. Bioactive metabolites from *Spilanthes acmella* Murr. Molecules 14, 850–867.
Salum, M.L., Robles, C.J., Erra-Balsells, R., 2010. Photoisomerization of ionic liquid ammonium cinnamates: one-pot synthesis-isolation of *Z*-cinnamic acids. Org. Lett. 12, 4808–4811.
Skehan, P., Storeng, R., Scudiero, D., Monks, A., Mcmahon, J., Vistica, D., Warren, J.T., Bokesch, H., Kenney, S., Boyd, M.R., 1990. New colorimetric cytotoxicity assay for anticancer-drug screening. J. Natl. Cancer Inst. 82, 1107–1112.
Su, B.-L., Zeng, R., Chen, J.-Y., Chen, C.-Y., Guo, J.-H., Huang, C.-G., 2012. Antioxidant and antimicrobial properties of various solvent extracts from *Impatiens balsamina* L. stems. J. Food Sci. 77, C614–C619.
Tabakman, R., Jiang, H., Shahar, I., Arien-Zakay, H., Levine, R.A., Lazarovici, P., 2005. Neuroprotection by NGF in the PC12 in vitro OGD model: involvement of mitogen-activated protein kinases and gene expression. Ann. NY Acad. Sci. 1053, 84–96.
Takaya, Y., Furukawa, T., Miura, S., Akutagawa, T., Hotta, Y., Ishikawa, N., Niwa, M., 2007. Antioxidant constituents in distillation residue of *Awamori spirits*. J. Agric. Food Chem. 55, 75–79.
Xie, X., Stahl, S.S., 2015. Efficient and selective Cu/nitroxyl-catalyzed methods for aerobic oxidative lactonization of diols. J. Am. Chem. Soc. 137, 3767–3770.
Yuan, L., Zhao, P.-J., Ma, J., Lu, C.-H., Shen, Y.-M., 2009. Labdane and tetranorlabdane diterpenoids from *Botryosphaeria* sp. MHF, an endophytic fungus of *Maytenus hookeri*. Helv. Chim. Acta 92, 1118–1125.
Zhang, S., Hu, D.-B., He, J.-B., Guan, K.-Y., Zhu, H.-J., 2014. A novel tetrahydroquinoline acid and a new racemic benzofuranone from *Capparis spinosa* L., a case study of absolute configuration determination using quantum methods. Tetrahedron 70, 869–873.